Calculating Molecular Spectra

Jonathan Tennyson and Steven Miller
Department of Physics and Astronomy, University College London, London WC1E 6BT

1 Introduction

Spectra, the absorption or emission of light at characteristic wavelengths, have long been known to provide accurate fingerprints of molecular species. Spectroscopic analysis is standard for characterizing species and for identifying and quantifying molecules in complex mixtures. It also provides information on such things as temperature and isotopic abundances. We are particularly interested in these properties as a diagnostic for 'cool' astronomical bodies. Astronomically, molecular spectra provide a unique handle on the physical conditions in environments such as giant molecular clouds, planetary atmospheres, and cool stellar atmospheres. As a counter example *infra red* spectroscopy is widely used in the petroleum industry to monitor everything from the oxidation of oils in engines to the composition of exhaust gases after combustion.[1]

The detailed information contained in the many transitions that characterize the spectrum of a molecule is a sensitive reflection of the underlying interactions within that molecule. Thus the rotational energy levels of a molecule are largely governed by the molecular geometry: microwave spectroscopy, the study of rotational transitions, has long provided the most accurate determination of molecular bond lengths. Conversely the vibrational energy levels of a molecule are determined by the ease with which the atoms can move relative to each other within the molecule: *infra red* spectroscopy, which covers the wavelengths of the strongest vibrational transitions, provides, at least in principle, detailed and often very accurate information on how the atoms in a molecule interact.

The interaction of atoms within a molecule is governed by the electronic potential energy surface of the system (see Section 2). Potential energy surfaces are important entities within chemistry as they determine not only spectra, but also reaction dynamics, transport properties, and interactions in the liquid and solid state. Although all these properties are sensitive to the potential, spectroscopy is undoubtedly the most accurate source of information on the potential. Unfortunately, except for diatomic molecules, there is no general method of extracting potentials from spectroscopic data. This leads to an alternative strategy. Potentials constructed by any means, from first principles application of quantum mechanics to guess work, are tested by using them to generate spectra which can be compared with observation. If the agreement is unsatisfactory the potential can be adjusted and the calculation repeated.

Recorded spectra, particularly for polyatomic molecules, are often very complicated. They can contain many thousands of lines each corresponding to transitions between unknown levels. The process of assigning such spectra involves ascribing degrees of vibrational and rotational excitation to both the initial and final levels involved in the transition. Often this is quite straightforward once a few assignments have been made but the first assignments may involve inspired guesswork and can be greatly aided by calculations. Similarly predictions of where the transitions can be found greatly aid the search for a particular species.

Calculations of molecular spectra are thus important for testing and developing potential energy surfaces, interpreting laboratory data, and predicting spectra. However, even for a three-atom molecule, such as water, at room temperature the spectrum can contain a very large number of transitions. The total absorption of light as a function of wavelength, which is called the opacity of the system, is an important property of many bodies including the Earth's atmosphere.

A detailed knowledge of the opacity of the atmosphere is required to model the greenhouse effect. The peak of the Sun's radiation is at optical wavelengths to which the Earth's atmosphere is largely transparent. The Earth is cooler which means that it re-emits radiation at longer wavelengths – mainly in the *infra red*. If this emission passes through the atmosphere then the earth will lose heat; if the atmosphere absorbs the emission then this heat is retained. This is a fine balance which is dependent on the components of gases in the atmosphere. Although CO_2 is well known as a greenhouse gas, many other atmospheric trace species such as methane, Chloro–Fluoro–Carbons (CFCs) and their derivatives, actually have a much greater potential to act as greenhouse gases. The generation of the many transitions involved in synthesizing opacities for these species is naturally handled computationally. We are currently embarking on such a project focusing on the behaviour of cool stellar atmospheres.

2 Potentials

As mentioned above, potential energy surfaces form a common strand running through practically all areas of physical chemistry. Actually the very existence of these surfaces relies on an approximation, albeit one which usually is valid.

Chemists generally consider molecules to be composed of electrons which are light and singly charged, and compound nuclei which are comparatively heavy (hydrogen is 1836 electron masses) and multiply charged. Given the large mass ratio, it is generally assumed that the electrons can relax instantaneously to any given nuclear geometry. It is within this framework, known as the Born–Oppenheimer approximation, that molecular potential energy surfaces can be defined. The potential energy for a particular nuclear configuration, generally denoted

Jonathan Tennyson studied Natural Sciences at King's College Cambridge (B.A. 1977). In 1980 he completed a Ph.D. in Theoretical Chemistry at Sussex University under the supervision of Professor John Murrell. He then spent two years at the University of Nijmegen, The Netherlands, as a Royal Society Western Exchange Fellow followed by three years at the SERC Daresbury Laboratory where he worked on calculations of photoionization and electron molecule scattering. He moved in 1985 to the Department of Physics and Astronomy at University College London and was promoted to Reader in 1991.

His current research interests include calculating the ro-vibrational spectra of molecules, the consequences of classical chaos on molecular spectra, electron (positron) molecule collision calculations, and the calculation of molecular data for astrophysics (including observational studies).

Jonathan Tennyson is the great, great grandson of Alfred Lord Tennyson.

Steven Miller gained B.Sc. (1970) and Ph.D. (1975) degrees from Southampton University. Two years at UMIST as research fellow and two at Sheffield University were followed by seven years working as a political journalist before he joined the Molecular Physics Group at University College London to work on ro-vibrational transitions of triatomic molecules, including H_3^+.

He has pioneered the use of H_3^+ *as an astronomical probe of planetary atmospheres and made the first identification of* H_3^+ *outside the solar system (in Supernova 1987A) in 1990.*

V, is a function only of the relative nuclear coordinates as the electronic motion is assumed to be fully adjusted to this geometry.

Potentials can be calculated using first principles quantum mechanics or *ab initio*, by choosing a set of internuclear separations, solving the resulting Schrödinger equation for the electronic motion and repeating the procedure until a grid of points has been generated. These points must then be fitted to some continuous function to produce a full surface. Solution of the electronic Schrödinger equation is a formidable problem in its own right but one which has advanced rapidly with theoretical developments and computer technology. It should be noted, however, that the generation of full *ab initio* potential energy surfaces for polyatomic molecules remains computationally expensive.

The traditional method of extracting potentials from observed spectra has been *via* force constants. These constants underpin a theory of vibrational motion which assumes the nuclei undergo only small amplitude motion. The force constants represent the derivatives of the potential at the equilibrium geometry of the molecule and as such give a very high order representation of the surface at one point rather than a global surface. There have been a number of suggestions as to which coordinates give the best extrapolation of the potential away from equilibrium. But no completely satisfactory solution exists.

An alternative method of obtaining potentials from experiment has been to make some initial guess at a potential function which contains parameters that can be optimized by comparison with experimental data. This procedure places great emphasis on the development of computationally efficient procedures for calculating spectra as this is the slowest step in the process. The method was first extensively used for atom–diatom van der Waals complexes such H_2–X and HCl–X (where X = He, Ne, Ar, Kr).[2,3] These weakly bound systems have the advantage that the relatively stiff diatomic vibrational mode can be neglected. The other vibrational modes undergo large amplitude motions which are poorly represented as an expansion about equilibrium. More recently this method has been applied to chemically bound systems such as water,[4,5] H_2S,[5] and HCN.[6]

3 Diatomic Molecules

Given a potential energy curve the calculation of rotation–vibration spectra for diatomic molecules is relatively straightforward. For these systems the potential energy surface and hence also the vibrational wavefunction is one dimensional. This makes visualization of both these functions straightforward. Similarly the degree of vibrational excitation in a diatomic is given by the number of times the wavefunction passes through zero. These zero amplitude points are called nodes.

A number of model potentials have been proposed for diatomics. These include harmonic, Morse, and Lennard-Jones 6—12 potentials. The first two of these are illustrated in Figure 1.

The harmonic potential is important not so much for its quantitative properties, but because most of the language used to interpret vibrational spectra is based upon it. Representing vibrational motion as harmonic oscillations is valid if the amplitude of these vibrational motions is small. In this approximation vibrational energy levels are evenly spaced. However, the harmonic model neglects all possibility of molecular dissociation. This introduces so called anharmonic effects which usually cause the spacing between vibrational levels to decrease. Of course vibrational motion becomes increasingly large amplitude as dissociation is approached.

The Morse potential, also shown in Figure 1, contains the basic properties of most diatomic molecules. It is strongly repulsive when the nuclei are close together, has a minimum at some intermediate distance and dissociates at long bond length. It is thus capable of representing basic anharmonic effects although for fully quantitative results more sophisticated functions are generally required.

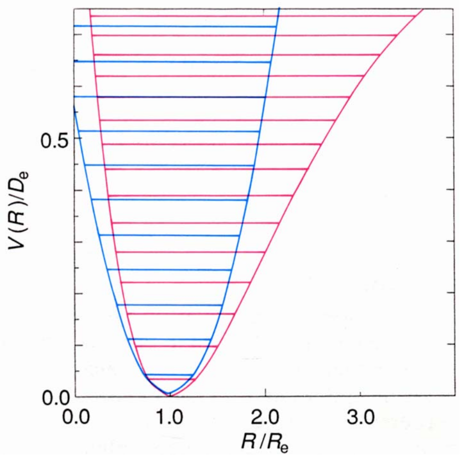

Figure 1 Potential energy curves, $V(R)$, for a diatomic with equilibrium bond length R_e and dissociation energy D_e. The blue curve is harmonic and the red curve is a Morse potential. Horizontal lines indicate vibrational energy levels. Both potentials have the same curvature (force constant) at $R = R_e$.

There are now many computational techniques for direct numerical integration of one-dimensional second-order differential equations of type encountered for diatomic systems. This means that, given a potential, the rotation–vibration energy levels of a diatomic system can be routinely obtained. This is in contrast to polyatomic systems.

4 Coordinate Systems for Polyatomic Molecules

If a molecule consists of N nuclei then $3N$ coordinates are required to describe the position of these nuclei in space. The translational motion of the molecule can be represented by the 3 coordinates of its centre-of-mass. Similarly for a non-linear molecule, rotational motion can be represented by a further 3 coordinates. This leaves $3N - 6$ ($3N - 5$ for a linear molecule) coordinates to represent the vibrational motion of the molecule. These are usually described as internal coordinates.

For diatomics the bond length of the molecule is also the natural internal coordinate of the system. Even for triatomic systems, however, there is no unique choice of internal coordinates which gives a good picture for all systems.

Traditionally so called normal coordinates have been used to represent the motions of polyatomic molecules. These coordinates are obtained as the solution of the multi-dimensional harmonic problem assuming that only harmonic terms are retained in the molecular potential. But these coordinates are unsatisfactory in many cases. This is because, given enough internal energy, all molecules undergo large amplitude vibrational motion which is not well represented within the harmonic approximation. In particular there is a technical problem that with these coordinates it is all too possible to leave the true domain of the problem. This is illustrated by Figure 1 where it can be seen that for high energies the harmonic potential crosses $R = 0$ and allows the vibrational wavefunction to sample negative bond lengths.

Normal coordinates have now been largely abandoned for accurate calculations on small molecules. Instead internal coordinates defined in terms of internuclear separations and associated angles are usually employed. Figure 2 illustrates 3 of many such triatomic coordinate systems.

The internuclear coordinates (r_1, r_2, r_3), Figure 2a, would appear a good coordinate choice for a number of triatomic systems. This is particularly so for the molecule H_3^+, discussed below, whose equilibrium geometry is an equilateral triangle and for which it is thus desirable to have coordinates reflecting the high symmetry of the system. Unfortunately these coordinates are inconvenient to work with as their allowed ranges are

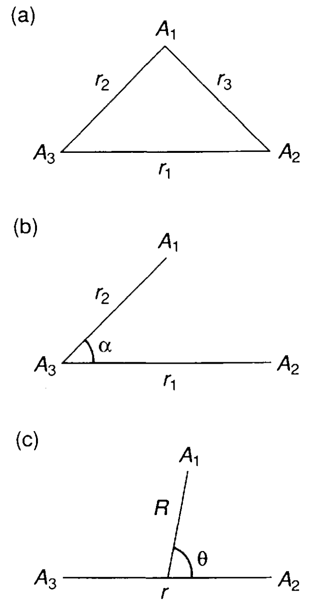

Figure 2 Internal coordinates for triatomic systems: (a) bond length coordinates (r_1, r_2, r_3); (b) bond length – bond angle coordinates (r_1, r_2, α); (c) scattering coordinates (r, R, θ).

linked by a series of triangulation relationships of the form $|r_1 - r_3| \leqslant r_2 \leqslant r_1 + r_3$. This makes numerical integration very difficult and as a consequence these coordinates are generally not used.

Bond length–bond angle coordinates (r_1, r_2, α), Figure 2b, give a good representation of many triatomics such as H_2O and H_2S. These coordinates have often been used for these molecules. Recently Radau coordinates, originally developed to study planetary motion about the Sun, have also been used for such systems. When the central atom is heavy, these coordinates are very similar to the bond length–bond angle coordinates but have the advantage that they yield a much simpler kinetic energy operator in the nuclear motion Hamiltonian.

Scattering coordinates (r, R, θ), Figure 2c, like Radau coordinates, also give a simple (diagonal) kinetic energy operator. These coordinates got their name from their use to represent atom–diatom collisions: the intersection of $\boldsymbol{r}$ and $\boldsymbol{R}$ being at the diatom centre-of-mass. They are appropriate not only for weakly bound atom–diatom van der Waals complexes but also for a molecule like HCN as the coordinates can link the equilibrium structure of the two linear isomers HCN and HNC.

Even if there is no coordinate system in which the vibrational motion is separable, it is still usual to talk about a molecule having $3N - 6$ vibrational modes. Like the internal coordinates, how these modes are chosen is not unique. The process of partitioning the vibrational energy between the vibrational modes, known as assignment, will be discussed below.

There are also many ways of defining the 3 coordinates that represent the overall rotational motion of the system. This is because these coordinate depend on how one fixes ('embeds') the x, y, and z axes to the molecule. Thus, for example, in the scattering coordinates of Figure 2c the z axis of the system is often embedded along either $\boldsymbol{r}$ or $\boldsymbol{R}$ depending on what is most appropriate for the system.

5 Hamiltonians

The equations of motion for N interacting particles, or their quantum mechanical equivalent given by the Hamiltonian, can easily be written down. However, the removal of translational motion, combined with coordinate transformations to internal coordinates and a particular axis embedding means the Hamiltonian itself must be transformed. Each time one defines a new set of internal coordinates or axis embedding it is necessary to construct a new Hamiltonian for the system. A general method for deriving these Hamiltonians has been developed by Sutcliffe[7] but its application is often algebraically messy.

Unfortunate as this may seem, there is a more serious problem. The very process of defining internal coordinates and axis embeddings introduces geometries into the Hamiltonian where it is badly behaved. For example, these badly behaved geometries, or singularities, are often encountered when a molecule becomes linear. In this case the system only has 2 instead of 3 rotational degrees of freedom and $3N - 5$ instead of $3N - 6$ vibrational modes. Special care is thus required for any bent molecule which samples linear geometries.

6 The Variational Principle

In its simplest form the Raleigh–Ritz Variational Principle states that for a given Hamiltonian operator the energy of any approximate wavefunction will always be greater or equal to the lowest (ground state) energy of the system. This theorem can also be extended to give upper bounds for the energy of excited states provided that the trial wavefunctions obey certain simple constraints.[8]

The Variational Principle has been a rock upon which much of quantum chemistry has been founded. It allows trial wavefunctions to be improved systematically with the best function being given unambiguously by the function with the lowest energy. Particularly powerful in variational calculations are basis functions. These allow the trial wavefunction to be expanded as linear combination of suitable functions:

$$\Psi(\boldsymbol{q}) = c_1\phi_1(\boldsymbol{q}) + c_2\phi_2(\boldsymbol{q}) + c_3\phi_3(\boldsymbol{q}) + \ \ldots \qquad (1)$$

The coefficients, given by the vector $\boldsymbol{c}$, can be varied until the best trial wavefunction is obtained. This procedure can be written in terms of matrices and is thus particularly well suited to computer implementations. These ('secular') matrices are diagonalized to yield the $\boldsymbol{c}$'s as eigenvectors and energies as eigenvalues.

In the secular matrix method, which is commonly used in all branches of quantum chemistry,[8] matrix elements are given by

$$H_{i,j} = \int \phi_i^* \hat{H} \phi_j \mathrm{d}\tau \qquad (2)$$

In this expression, $\boldsymbol{H}$ is the secular matrix, $\hat{H}$ the Hamiltonian for the system and the ϕ's are the basis functions. The integral runs over all space with $\mathrm{d}\tau$ being the appropriate volume element. Usually at least some of the integrals involved in this expression have to be evaluated using numerical quadrature. Provided the matrix elements are real, the secular matrix is symmetric (*i.e.* $H_{i,j} = H_{j,i}$).

For vibrational problems suitable basis functions include solutions of the harmonic oscillator and Morse problems discussed in Section 3. The basis sets required to give a complete representation of the vibrational motion are always infinite. One's aim is therefore to make a judicious choice of functions so that only a few are required to give a good representation of the wavefunction. Convergence is reached when the use of additional functions only leads to an insignificant lowering of the energy.

For rotational degrees of freedom the situation is simpler. For a given rotational quantum number, J, it is only necessary to have $(2J + 1)$ functions to represent the rotational wavefunction fully. These functions, known as Wigner rotation matrices,[9] can thus be used to expand any rotational problem and their use is universal.

For triatomics, variational calculations performed using basis sets give a computer time requirement which is almost always determined by the size of the secular matrix that needs diagonalizing. A technique which has proved highly successful in molecular vibration–rotation calculations is the application of the Variational Principle in several steps.[11] In such procedures a problem of reduced dimension is solved using a basis set expansion and the solutions of this problem used as the basis for a higher dimensional problem. If the reduced problem is well chosen then only a minority of its solutions are needed to obtain converged results for the full problem. This can lead to massive savings in computer time. Such methods have allowed the solution of many problems which would otherwise be beyond the scope of current computers.

7 Molecular Properties

The most obvious results obtained from solving the vibration–rotation problem are the (approximate) wavefunction of the system and its associated energy levels. However, quantum mechanics tells us that with the wavefunction we can calculate all other knowable properties of the system. Of particular interest in this context are the intensities of the transitions between the various states of the system.

Most common transitions which involve absorbing or emitting light are driven by dipoles. Thus the intensity of a pure rotational transition is proportional to the square of the permanent dipole of the molecule. For vibrational transitions the important property is the change in the dipole moment in the vibrational coordinate being excited. In the harmonic model of molecular vibrations this is simply given by the derivative of the dipole at the equilibrium geometry of the molecule. However, more accurate calculations require a knowledge of the dipole as a function of the internal coordinates of the molecule, as well as the wavefunction of the initial and final state. In fact, because the dipole is a vector, 3 surfaces (2 for planar molecules such as triatomics) are required.

Transition dipoles not only give the strength of individual absorption or emission features, they can also be used to give fluorescence lifetimes of excited states. (Fluorescence lifetime is the average length of time an excited state will survive before decaying to a lower level by the spontaneous emission of a photon.)

Dipole surfaces can also be used to give vibrationally resolved dipole moments. Similarly any other property of the molecule which is geometry dependent, such as bond lengths, rotational constants, or polarizabilities, can be obtained for different states of the system by using the wavefunction to do the appropriate average.

The wavefunction of the system can always be labelled by the total angular momentum of the system, J, as this is a constant of motion. However it is usual to label molecules by the number of quanta of vibrational excitation in each vibrational mode of the system. Such labelling is often based on a harmonic model of the system and is always approximate. The process of attaching these labels is called assignment. Assigning levels is important as a wealth of detailed understanding of how systems behave has been developed in terms of these assignments. Furthermore, as experiments never record all transitions for a system, assignments are crucial in any comparison between theory and experiment.

Usually low-lying levels can be assigned without difficulty either by studying energy patterns or by using the coefficients in the basis set expansion. For higher-lying levels making assignments can be very much trickier. The density of vibrational states increases with energy, making energy differences unreliable, and individual states may no longer be dominated by a single basis function.

Another technique for making assignments, used extensively by us, is visual inspection of the wavefunction. This is normally achieved by making contour plots of the wavefunction or cuts through the wavefunction – see Figures 3 and 4. States that can easily be assigned are characterized by nodes in the wavefunction which give a simple grid pattern; some examples are given in Figures 3a and 4a. For higher-lying states there may be no assignable nodal structure. This may be because inappropriate coordinates have been used for preparing the contour plots or because the state may be inherently unassignable.

Unassignable states can usually be associated with energy regions for which classical solutions of the same problem are chaotic. How classical chaos manifests itself in quantal systems remains a controversial subject and is beyond the scope of this article. However, one property that is observed in both mechanics is that even above the transition to classical chaos, some assignable solutions are found. Figure 4b depicts wavefunctions of the H_3^+ molecular ion whose energies are well above the classical transition to chaos. For three states the wavefunction

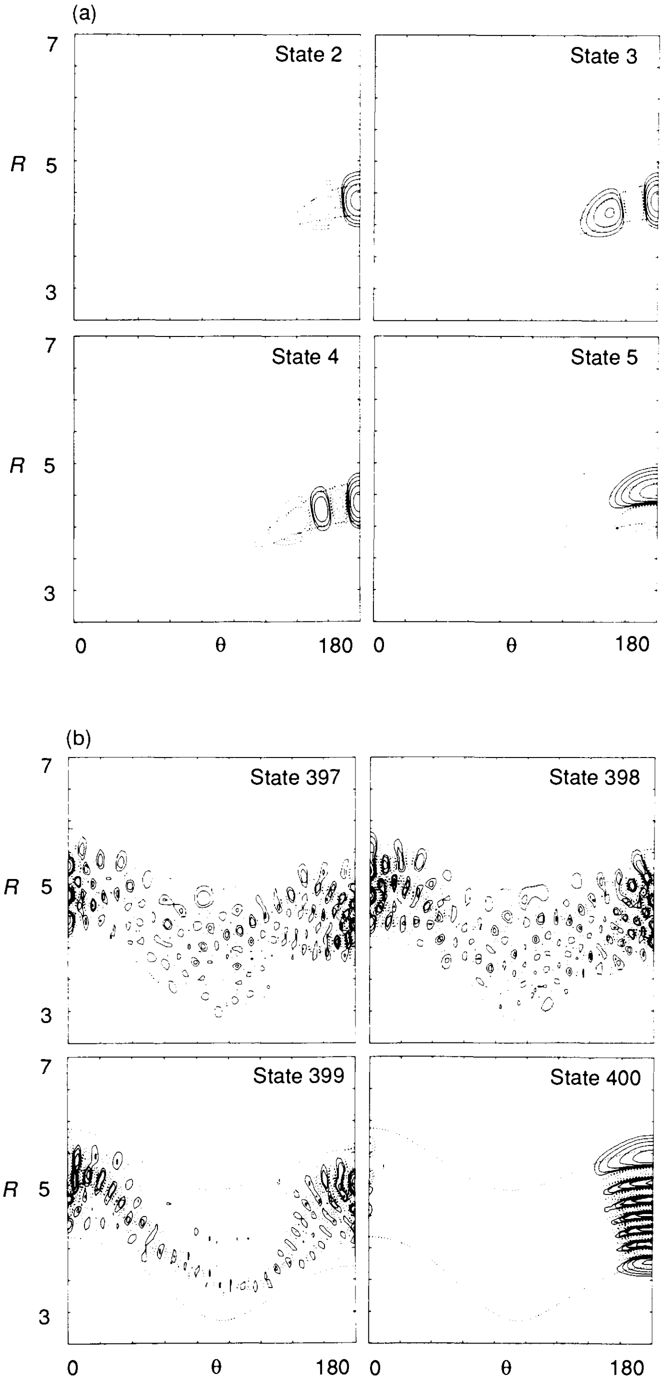

Figure 3 Contour plots of the wavefunction of 8 vibrational states of LiCN: (a) low-lying states, (b) highly excited states. The plots are in scattering coordinates with the CN bond length, r, frozen at its equilibrium value. $\theta = 180°$ for linear LiNC and 0° for linear LiCN. Solid lines enclose regions where the wavefunction is positive and dashed lines regions of negative amplitude. Nodal planes occur where the wavefunction has zero amplitude. The outer dotted curves represent the limits of the classically accessible potential for each state – in quantum mechanics the wavefunction can tunnel into this region. (After J. R. Henderson and J. Tennyson, *Mol. Phys.*, 1990, **69**, 639.)

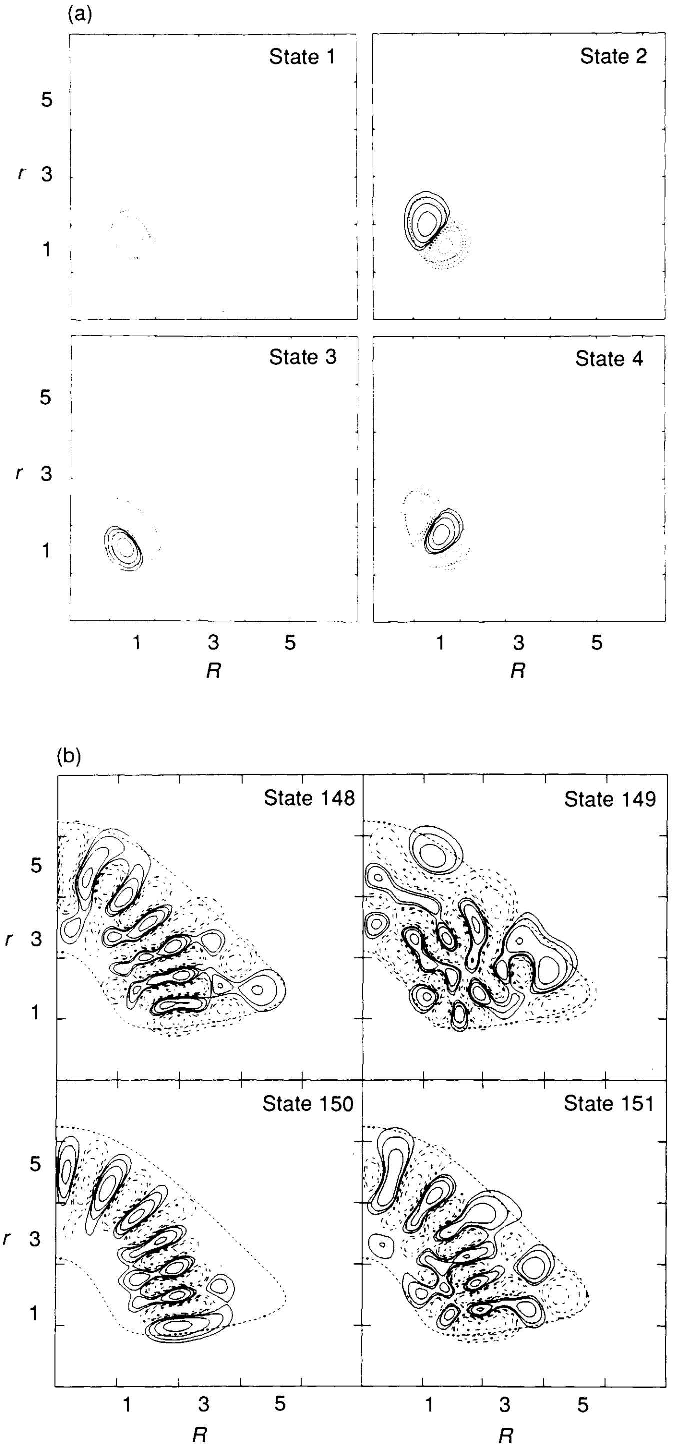

Figure 4 Contour plots of the wavefunction 8 vibrational states of H_3^+: (a) low-lying states; (b) highly excited states. The plots are in scattering coordinates with θ frozen at 90°. The contours are as for Figure 3. (After J. R. Henderson and J. Tennyson, *Chem. Phys. Lett.*, 1990, **173**, 133.)

appears irregular. State number 150 has a clearly defined nodal structure spread along a half horseshoe shape – and is called a horseshoe state.[10]

The energy levels of the system can also be used to give other properties of the system. The most obvious of these is the partition function, the factor which normalizes the Boltzmann distribution of molecules into particular states. The partition function is needed if one wants to synthesize spectra as a function of temperature.

8 Sample Results

Variational calculations have been performed on many triatomic and some tetratomic molecules. We choose a few of these to give a flavour of what can be achieved.

8.1 H_3^+: from Jupiter to Chaos

Perhaps the most exciting project that we have been involved in concerns the fundamental molecular ion H_3^+. This seemingly simple molecule consists of 2 electrons and 3 protons. Its relatively simple electronic structure means that potential energy surfaces for this molecule can be calculated more accurately by using first principles quantum mechanics[12] than by analysing experimental data. This situation is probably unique for a polyatomic.

H_3^+ is rapidly formed when H_2 is ionized by the exothermic reaction

$$H_2 + H_2^+ \rightarrow H_3^+ + H \qquad (3)$$

As H_2 is the most abundant molecule in the universe, there are many astronomical situations where H_3^+ is expected, although it remains largely unobserved. Similarly H_3^+ is easily formed in the laboratory using a hydrogen discharge.

H_3^+ is an equilateral triangle in its equilibrium geometry. However, because of its light nuclei, H_3^+ undergoes large amplitude vibrational motion. We have performed a series of variational calculations on this molecule in an attempt to aid both laboratory assignment of the complicated *infra red* spectra of this molecule and its astronomical detection.

These calculations took a new significance following observations of Jupiter by Drossart *et al.*[13] These workers were studying a known hot region near Jupiter's south pole. In particular they were looking for very weak transitions due to molecular hydrogen. They observed these lines but at the same time saw 28 other, unexpected, transitions which they were unable to explain. It transpired that a spectrum like this had been observed at the Herzberg Institute of Astrophysics in Ottawa but only assigned as a result of these observations.[14] Because it was thought that the experimental spectrum was probably due to H_3^+ our calculations were enlisted.

Figure 5 gives a comparison of our calculated spectrum and that observed by Drossart *et al.* Note that the observed line at 4721 cm^{-1} is due to H_2. The agreement is striking. Our calculations match the observed lines positions to within about 0.02%. There are a number of surprising aspects of this first extraterrestrial observation of H_3^+. The actual transitions involve jumps of two vibrational quanta. Conventional wisdom is that such transitions should be very weak, but the floppiness of H_3^+ makes the two-quanta transitions nearly as strong as the fundamental or one-quantum transition, which has since also been observed in Jupiter.[15] Another surprising outcome of this observation was that the observed spectrum could only be modelled by H_3^+ with a temperature in the region of 1000 K. This is a high temperature for a planet whose body is at about 200 K.

The observation of H_3^+ in Jupiter has stimulated a very active area of astronomical research studying H_3^+ in Jupiter and elsewhere. This will be the subject of another article by us in this journal.

While the electronic properties of H_3^+ may be fairly simple, its nuclear dynamics are extremely rich. Attention was focused on this by the observation of a very unusual spectrum by Carrington and co-workers.[16] This experiment prepared H_3^+ in a discharge and probed the resulting ions with an *infra red* laser. A mass spectrometer was then used to monitor if any protons were produced by photodissociation.

Photodissociation is a common technique for investigating molecular systems and the resulting spectra are often quasi-continuous with maybe rather lumpy features. The spectrum obtained by Carrington and co-workers was extraordinary for two reasons. The energy of the laser was only a small fraction of that required to dissociate the ground state of the H_3^+ and the

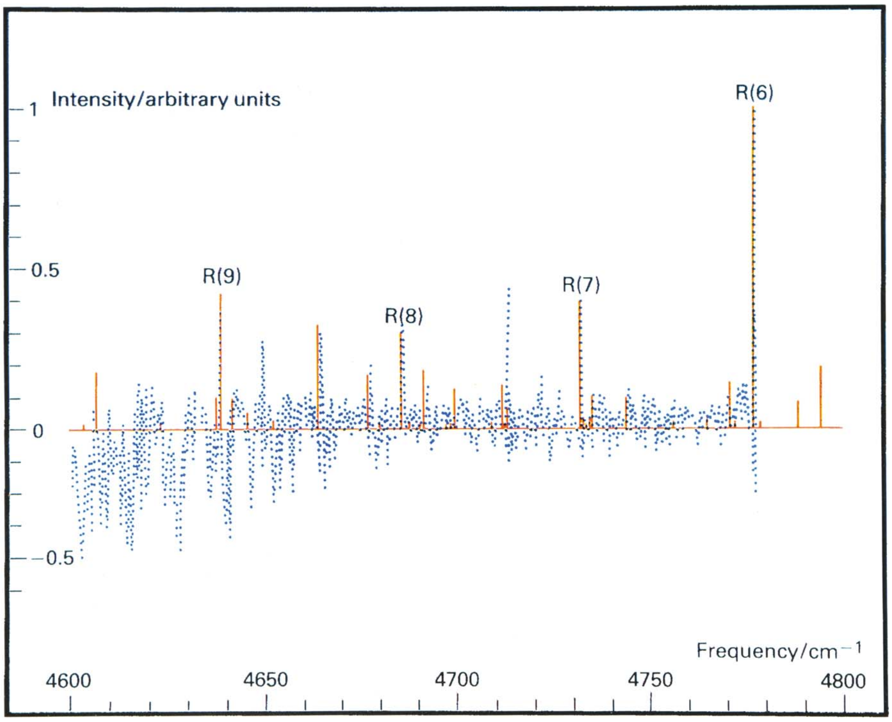

Figure 5 Observed (blue) and simulated (red) emission spectrum from Jupiter's southern polar region. The labels identify the rotational levels of H_3^+ involved: $R(J)$ is a $J + 1 \leftarrow J$ transition.
(Reproduced by permission from *Chem. Br.*, 1990, **26**, 1069.)

spectrum, taken over a small range of wavelengths, contained over 26 000 narrows lines.

This spectrum, occurring as it does right at the dissociation limit of the molecule, presents a formidable challenge to theory. Further analysis of the experiments showed that the protons generally left the molecule with more energy than they got from the laser. This could only be rationalized by placing *both* the initial and final state of the system above the dissociation limit of the molecule. Such quasibound states, physicists call them shape resonances, are well known although such a profusion of them is unusual. They result from rotational excitation of the molecule which causes the potential to be distorted by a hump or barrier to dissociation. The molecule can get trapped behind this hump, but because of quantum mechanical tunnelling, the state only remains trapped for a finite time. The Uncertainty Principle means that states which are trapped only for a short time have large uncertainty in their energy and appear as broad lines in any spectrum. All the observed H_3^+ lines are narrow suggesting that they are associated with long-lived states.

The dissociation spectrum of H_3^+ as observed has little structure. However, if a spectrum is synthesized by broadening the observed lines, then the spectrum collapses to 4 regularly spaced features. This intriguing piece of information has been a challenge to theoreticians. Classical analysis of the H_3^+ system suggests that the molecule is almost totally chaotic once the molecule has chance to become linear. Such geometries become accessible at energies about one third of the way to dissociation. In chaotic systems it is usual for some solutions ('trajectories') to behave in a regular or quasiperiodic fashion. Classical mechanicians argue that the structure in the H_3^+ spectrum is caused by some underlying regular motion with the many individual transitions being a reflection of the chaotic nature of the system. This explanation leaves two questions. What is the underlying regular motion and how does the fact that H_3^+ obeys quantum and not classical mechanics alter this picture?

One proposal for the regular motion is that the atoms undergo a 'horseshoe' motion.[10] In scattering coordinates, see Figure 2c, this motion can be described in terms of the coupled motions of r and R with θ fixed at 90°. As R goes towards zero, r becomes large as the other two atoms move apart to allow the central atom through. As R moves away from zero, r decreases again. Plotting this motion as a function of r against R, where R has the range $-\infty \rightarrow +\infty$, gives a horseshoe shape.

Quantum mechanical calculations on these high energy regions are very difficult, not least because the density of states rises rapidly with energy. However modern supercomputers and the adaptation of the variational procedures described above to use methods based on finite elements rather than basis functions have allowed such calculations to be attempted. So, for example, a quantal calculation has recently estimated the position of *every* bound vibrational state of H_3^+.[17] Figure 4 shows wavefunctions produced by these calculations. The states of H_3^+ are plotted in scattering coordinates with θ fixed at 90°. In these plots R has the range $0 \rightarrow +\infty$. State 150 has a (half) horseshoe-like shape and is regular in the sense that nodes can easily be counted. The other states in Figure 4b, which are typical of many states in the high energy region, have irregular structures.

Although there is clear evidence for horseshoe states in the quantum mechanical calculations, their exact role in the H_3^+ dissociation spectrum remains controversial. So far the quantal calculations have not been sophisticated enough to generate actual spectra: in particular no-one has managed to study the effect of rotational excitation on the high-lying states. A decade after the first *infra red* photodissociation spectrum of H_3^+ was recorded there is still clearly some way to go before it is fully understood.

8.2 Van der Waals Complexes: Ar$-$N$_2$

Van der Waals bonding is the weak attraction which results from charge clouds adjusting to each others instantaneous fluctuations. It is the weakest of the chemical bonds and thus van der Waals molecules are only very weakly bound.

Van der Waals complexes are thus aggregates of stable, often closed shell, molecules. The most studied triatomic van der Waals systems are the complexes formed between the Noble gases (He, Ne, Ar . . . .) and diatomics such as H_2, HF, HCl, and N_2. These systems have been prototypical in the development of variational methods. This is because their flat potential energy surfaces mean that the concept of vibrational motion as a (small) displacement from an equilibrium geometry is unhelpful. Internal coordinates, particularly scattering coordinates, have thus been used for some time for van der Waals complexes.

As mentioned earlier, the wealth of experimental data on certain van der Waals systems has meant that empirical potential energy surfaces have been derived for a number of complexes by performing cycles of calculation which involve guessing the surface, calculating the transition frequencies predicted by the surface, comparing with experiment, and repeating the procedure until a satisfactory surface is produced.[3] Recently an attempt has been to use a similar procedure to generate a dipole surface for the Ar$-$N$_2$ complex.[18]

For Ar$-$N$_2$ the experimental spectrum was obtained in the *infra red* by using wavelengths in the region of the N$_2$ vibrational fundamental.[19] As excitation of the vibrational mode of isolated N$_2$ is forbidden, this experiment is sensitive to those N$_2$'s which are part of a complex. Furthermore the transitions do not occur exactly at the frequency of the forbidden N$_2$ transitions because vibrational modes of the van der Waals complex can also be excited. The spectrum thus has several features, all of which are superimposed on a broad continuous background due to pressure broadening. Pressure broadening is the result of using relatively high pressures to produce the van der Waals complexes meaning that the molecules in the experimental cell can no longer be considered as isolated.

The experiments on Ar$-$N$_2$ were performed at liquid nitrogen temperatures of about 77 K. For a van der Waals complex this is hot and means that for Ar$-$N$_2$ all levels are thermally occupied. The result is that instead of consisting of a series of discrete lines, the experimental spectrum comprises a number of features each containing many transitions. Indeed the calculations found that the strongest individual transitions were ten times weaker than the features in the experiment. It was thus necessary to consider some 15 000 transitions in synthesizing the spectrum. These were obtained by calculating all vibration–rotation states of the system which lie below the dissociation limit of the complex.

Figure 6 compares the calculated and experimental spectra for the Ar$-$N$_2$ complex. The agreement is not spectacular but the comparison contains a wealth of information about the potential used for the calculations and the interpretation of the experiment. For instance, the broad shoulder in the calculated spectrum 7 cm^{-1} from the N$_2$ fundamental frequency (taken at the origin on the figure) is almost certainly a genuine feature which was lost in the process of removing the background due to pressure broadening from the observed spectrum. Conversely, the misalignment of the peaks marked S(0) is due to the potential energy surface used in the calculation. It would appear the potential for the Ar to move about the N$_2$ was not flat enough in the low-energy region. It will also be noticed that the observed spectrum has a much greater extent than the calculated one. This is because the calculations only considered truly bound states of the system, whereas the higher frequency features are due to quasibound states trapped behind rotational humps in the potential.

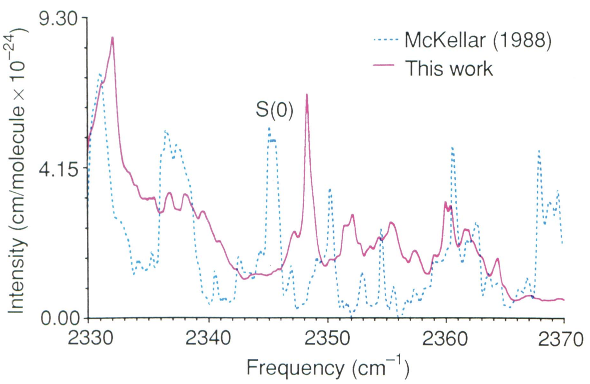

Figure 6 Observed (blue) and simulated (red) *infra red* absorbtion spectrum of the Ar$-$N$_2$ van der Waals complex. Both spectra are for a temperature of 77 K and a density of 1.7 amagat.
(After García Allyón *et al.*, *Mol. Phys.*, 1990, **71**, 1043.)

8.3 Potential Energy Barriers: Isomerization in LiCN

Many molecules are found to have more than one stable structure. These different structures are called isomers and in general become more common as the number of atoms in a molecule increases since this also increases the number of candidate structures. Some triatomic systems exist as different isomers. For example hydrogen cyanide is found with two linear structures. Indeed, an unresolved astrophysical problem is why HNC is almost as abundant in interstellar clouds as its much more stable HCN isomer.

Quantum chemical calculations have predicted that both linear forms of LiCN are also stable.[20] However, in this case the LiNC isocyanide is predicted to be the more stable form. This has been confirmed by microwave experiments.[21] Although HCN has been the subject of many variational calculations (*e.g.* ref. 6), LiCN is actually easier to work on. This is because in HCN the H$-$CN stretching mode is at a similar frequency to the C$-$N stretch. The heavier Li atom means that the high frequency C$-$N mode is approximately decoupled from the other vibrational modes in the system. Furthermore, the theoretical barrier between the two linear isomers of LiCN is small, only 3500 cm^{-1} (0.4 eV) or less than 5 quanta of the Li$-$CN stretch. As the LiCN is heavily ionic, the potential can be thought of as being Li$^+$ orbiting CN$^-$ with only a secondary sensitivity to the actual orientation of the CN$^-$.

LiCN has thus been the subject of a series of calculations all of which have frozen the CN motion. Within this model, the 65th state of the system is already in the region of the barrier. As recent calculations[22] have obtained wavefunctions for the lowest 900 states of the system, the behaviour of the system below the barrier, in the region of the barrier, and well above the barrier can be studied.

Plots of low-lying and high-lying states of LiCN are given in Figure 3. The lower states can all be easily assigned by their nodal patterns. However, as more energy is put into the Li$-$CN bending motion, the states become increasingly irregular. It is the bending motion which samples the isomerization barrier. The potential in this region is of course highly anharmonic and thus the assignments, based as they are on a harmonic picture of molecular vibrations, rapidly break down.

Above the barrier to isomerization an increasing proportion of states (more than 90% above state 400) have a highly irregular appearance and cannot be assigned. However, in this region there are series of states with clear nodal patterns. Perhaps the most pronounced of these series is the overtones of the isocyanide Li$-$CN stretch. These states go throughout the region studied. Thus state 400, depicted in Figure 3b, has 12 quanta of stretch.

An interesting and topical question is how the many irregular states in a system such as LiCN would manifest themselves in observed spectra. Calculations of the conventional absorption spectrum of the molecule in its ground vibrational states show few unusual features. This is because the spectra are dominated by excitations of the Li$-$NC stretching mode. The ionic nature of the molecule means that this mode has a large dipole which leads to very intense transitions. Similar behaviour has been observed experimentally for HCN.

A more revealing picture of the behaviour of the excited states of LiCN is obtained by considering their fluorescence lifetimes.[23] This is illustrated in Figure 7 which has an interesting structure: the assigned ('LiNC regular') states fall into a number of series. One series, for which the lifetime decreases with excitation, all have no stretching excitation and increasing quanta of bending energy. Conversely the other series are for 1, 2, 3, and 4 quanta of stretching excitation respectively, with the lifetime getting shorter as the degree of stretching excitation

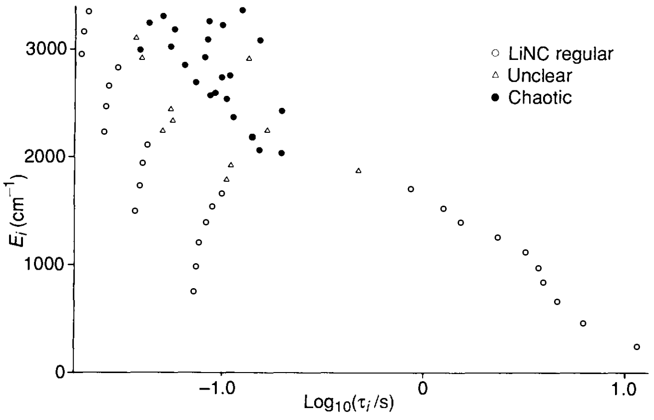

Figure 7 Fluorescence lifetime of excited vibrational states of LiNC with $J = 0$. E_i is the energy of each state relative to the LiNC ground states. Assignments as 'regular' or 'chaotic' were made by analysing contour plots of the wavefunctions such as those given in Figure 3. (Reproduced by permission from *Chem. Phys*, 1986, **104**, 399.)

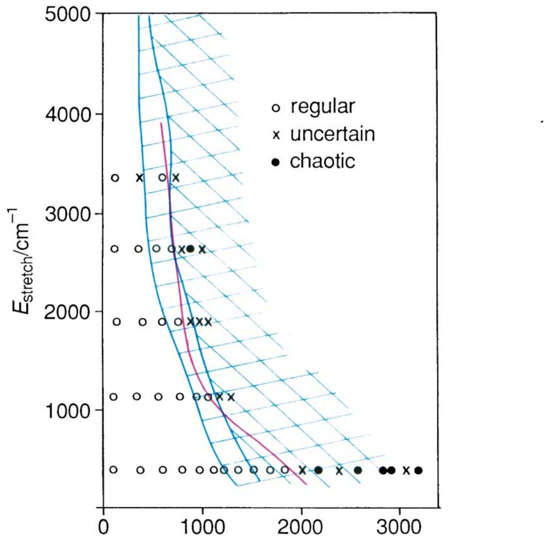

Figure 8 Comparison of the quasiperiodic (blank) – chaotic classical domain (hatched in blue) with 'regular' – 'chaotic' quantum states (red) for LiNC. Classical results were obtained by starting 50 trajectories with the energy indicated in the stretch and bend coordinates. Quantal results were obtained by partitioning energy between stretching and bending modes. This cannot be done for most 'chaotic' states which therefore do not appear on the figure.
(After J. Tennyson and S. C. Farantos, *Chem. Phys.*, 1985, **93**, 237.)

increases. Within each series, increasing the bending excitation leads to slightly longer lifetimes.

All this can be understood by remembering that because of its ionic nature the transitions in LiCN are very strong for stretching states. Thus any excited state which can do so decays rapidly by losing a quantum of stretch. Conversely decaying by losing one or more quanta of bending excitation is slow. However, as the molecule is excited there is an increase in bend–stretch mixing. This means that the higher bending states take on a small but increasing stretch character which shortens their lifetime whereas increasing the bending character of the stretch excited states lengthens their lifetime.

As the states become more excited the bend–stretch interaction becomes stronger. This leads to a host of states that have distorted wavefunctions which defy assignment. It also leads to a situation where all states have rather similar fluorescence lifetimes as represented by the clump of unassigned ('chaotic') states in Figure 7.

Analysis of classical calculations on LiCN shows that bending excitation is the main cause of chaotic behaviour in the system.[24] Indeed regular ('quasiperiodic') stretching states can be found over a wide energy range, possibly all the way to dissociation, provided that the bending excitation is kept low. Similar analysis of the quantal results[24] show again that regular stretching states can be found over an extensive energy range, see state 400 of Figure 4b for example.

A direct quantitative comparison of classical and quantal results is given by Figure 8. In this figure the energy is apportioned to either stretch or bending. The resulting state/trajectory is then assigned as either regular/quasiperiodic or irregular/chaotic and the appropriate entry made. It is clear that there is a wide measure of agreement between the predictions in the two mechanics although the onset of irregular quantum states occurs at a slightly higher threshold energy. This behaviour has been called 'quantum sluggishness'.

9 Conclusions

In this article we have given a brief review of how one performs vibration–rotation calculations on small molecules. We have tried to explain why these calculations are important and to give the scope of problems that can be addressed with these calculations by the discussion of some sample results. It will be noted that all the problems discussed are for triatomic molecules. In two of these cases the calculations involved finding *all* the bound states of the system – all the vibrational states of H_3^+ and all the vibrational and rotational states of $Ar{-}N_2$. These and most other variational calculations on triatomics can now be performed so accurately that the major source of error is the potential energy surface used for the calculation. This is still true for the most accurate vibration–rotation calculations available, *viz.* our own on H_3^+, which reproduce a range of experimental data with an error of about 1 part in 5000.

The advent of variational vibration–rotation calculations has really opened the way for serious and systematic theoretical analysis of the highly-excited states triatomic systems. Such states, as implied by the discussion of the H_3^+ and LiCN problems, are often found at energies where classically one finds chaos. What the exact consequences of this are for quantum mechanical wavefunctions or indeed spectroscopy is still a matter for considerable speculation. At least theoreticians now have the necessary tools in their armoury to tackle such problems.

Our discussion has concentrated almost exclusively on triatomic molecules. This does not imply that larger molecules are without interest. Quite the contrary, these systems are extremely challenging. A number of variational calculations on tetratomic systems have now been performed. The computational aspects of the tetratomic problem are rather different than for triatomics.

Although it has not been considered here, in order to form the matrix elements necessary to construct the secular matrix, it is necessary to integrate over the coordinates of the problem. If any arbitrary potential function is to be used, this integration must be done numerically in $3N - 6$ dimensions. It turns out that for triatomic systems ($N = 3$) this integration is much less computationally demanding than the later step in the calculation of diagonalizing the secular matrix. For tetratomic system ($N = 4$), 6D numerical integration must be performed. As the number of integration points increases roughly as M^{3N-6}, even a modest number of points in each dimension such as $M = 10$ leads to a thousandfold increase in computer time requirements. It is clear that any serious advance in the area of calculating spectra for larger molecules using variational procedures must somehow first break this integration bottleneck.

Acknowledgements. We thank our various collaborators, particularly James Henderson and Brian Sutcliffe, from whose work we have quoted freely. We also gratefully acknowledge funding from the Science and Engineering Research Council, the EEC, the British Council, the Research Corporation Trust, and NATO.

10 References

1 J. Birnie, *Spectrosc. World*, 1991, **3(3)**, 12.

2 R. J. Le Roy and J. S. Carley, *Adv. Chem. Phys.*, 1980, **42**, 353.

3 J. M. Hutson, *Annu. Rev. Phys. Chem.*, 1990, **41**, 123.

4 P. Jensen, *J. Mol. Spectrosc.*, 1989, **133**, 438.

5 E. Kauppi and L. Halonen, *J. Phys. Chem.*, 1990, **94**, 5779.

6 S. Carter, N. C. Handy, and I. M. Mills, *Proc. R. Soc. London, Ser. A*, 1990, **332**, 309.

7 B. T. Sutcliffe, in 'Methods in Computational Chemistry', Vol. 5, ed. S. Wilson, Plenum, (in press).

8 R. McWeeny, 'Methods of Molecular Quantum Mechanics', 2nd edition, Academic, London, 1989, Chapter 2.

9 R. N. Zare, 'Angular Momentum', Wiley, 1990.

10 J. M. Gomez Llorente and E. Pollak, *J. Chem. Phys.*, 1988, **88**, 1195; 1989, **90**, 5406.

11 J. Tennyson, S. Miller, and J. R. Henderson, in 'Methods in Computational Chemistry', Vol. 5, ed. S. Wilson, Plenum, (in press).

12 W. Meyer, P. Botschwina, and P. G. Burton, *J. Chem. Phys.*, 1986, **84**, 891.

13 P. Drossart, J.-P. Maillard, J. Caldwell, S. J. Kim, J. K. G. Watson, W. A. Majewski, J. Tennyson, S. Miller, S. Atreya, J. Clarke, J. H. Waite Jr., and R. Wagener, *Nature (London)*, 1989, **340**, 539.

14 W. A. Majewski, P. A. Feldman, J. K. G. Watson, S. Miller, and J. Tennyson, *Astrophys. J.*, 1989, **343**, L51.

15 S. Miller, R. D. Joseph, and J. Tennyson, *Astrophys. J.*, 1990, **360**, L55.

16 A. Carrington, J. Buttenshaw, and R. A. Kennedy, *Mol. Phys.*, 1982, **45**, 753; A. Carrington and R. A. Kennedy, *J. Chem. Phys.*, 1984, **81**, 91.

17 J. R. Henderson and J. Tennyson, *Chem. Phys. Lett.*, 1990, **173**, 133.

18 A. García Allyón, J. Santamaria, S. Miller, and J. Tennyson, *Mol. Phys.*, 1990, **71**, 1043.

19 A. R. W. McKellar, *J. Chem. Phys.*, 1988, **88**, 4190.

20 R. Essers, J. Tennyson, and P. E. S. Wormer, *Chem. Phys. Lett.*, 1982, **89**, 223.

21 J. J. van Vaals, W. L. Meerts, and A. Dymanus, *Chem. Phys.*, 1984, **77**, 4061.

22 J. R. Henderson and J. Tennyson, *Mol. Phys.*, 1990, **69**, 639.

23 J. Tennyson, G. Brocks, and S. C. Farantos, *Chem. Phys.*, 1986, **104**, 399.

24 J. Tennyson and S. C. Farantos, *Chem. Phys.*, 1985, **93**, 237.